Article

Cell

Human Adaptation of Ebola Virus during the West African Outbreak

Graphical Abstract

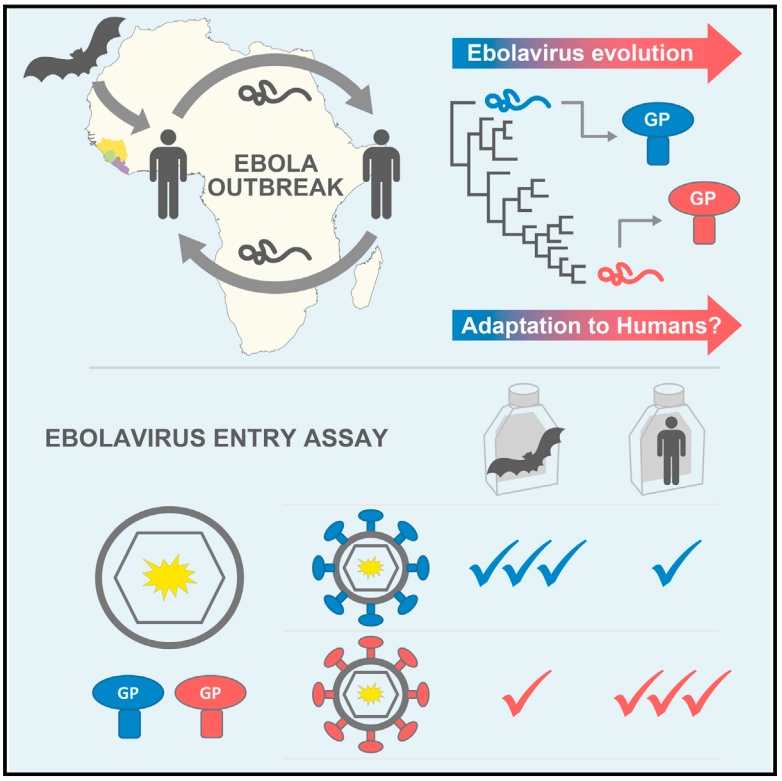

Highlights

- EBOV adapted to humans during the West African outbreak
- Amino acid substitutions in the EBOV glycoprotein increase human cell tropism
- The same glycoprotein amino acid substitutions decrease tropism for bat cells

Authors

Richard A. Urbanowicz,
C. Patrick McClure,
Anavaj Sakuntabhai, ..., Félix A. Rey,
Etienne Simon-Loriere, Jonathan K. Ball

Correspondence

etienne.simon-loriere@pasteur.fr (E.S.-L.),
jonathan.ball@nottingham.ac.uk (J.K.B.)

In Brief

The Ebola virus acquired amino acid substitutions in its glycoprotein that increased its tropism for human cells during the West African outbreak of 2013–2016.

Urbanowicz et al., 2016, Cell *167*, 1079–1087
November 3, 2016 © 2016 The Authors. Published by Elsevier Inc.
http://dx.doi.org/10.1016/j.cell.2016.10.013

CellPress

Article

Cell

Human Adaptation of Ebola Virus during the West African Outbreak

Richard A. Urbanowicz,[1,2] C. Patrick McClure,[1,2] Anavaj Sakuntabhai,[3,4] Amadou A. Sall,[5] Gary Kobinger,[6,7,8,13,14] Marcel A. Müller,[9] Edward C. Holmes,[10] Félix A. Rey,[11,12] Etienne Simon-Loriere,[3,4,*] and Jonathan K. Ball[1,2,15,*]

[1]School of Life Sciences, The University of Nottingham, Nottingham NG7 2RD, UK
[2]NIHR Nottingham Digestive Diseases Biomedical Research Unit, The University of Nottingham, Nottingham University Hospitals NHS Trust, Nottingham NG7 2UH, UK
[3]Functional Genetics of Infectious Diseases Unit, Institut Pasteur, 75724 Paris Cedex 15, France
[4]Centre National de la Recherche Scientifique, Unité de Recherche Associée 3012, 75015 Paris, France
[5]Arbovirus and Viral Hemorrhagic Fever Unit, Institut Pasteur de Dakar, BP 220 Dakar, Senegal
[6]Special Pathogens Program, National Microbiology Laboratory, Public Health Agency of Canada, Ottawa, ON K1A 0K9, Canada
[7]Special Pathogens Program, National Microbiology Laboratory, Public Health Agency of Canada, Winnipeg, MB R3E 3R2, Canada
[8]Department of Medical Microbiology, Faculty of Medicine, University of Manitoba, Winnipeg, MB R32T 2N2, Canada
[9]Institute of Virology, University of Bonn Medical Center, 53127 Bonn, Germany
[10]Marie Bashir Institute for Infectious Diseases and Biosecurity, Charles Perkins Centre, School of Life and Environmental Sciences and Sydney Medical School, The University of Sydney, Sydney, NSW 2050, Australia
[11]Institut Pasteur, Département de Virologie, Unité de Virologie Structurale, 75724 Paris Cedex 15, France
[12]Centre National de la Recherche Scientifique, Unité Mixte de Recherche 3569, 75724 Paris Cedex 15, France
[13]Present address: Département de microbiologie-infectiologie et d'immunologie, Université Laval, QC G1V 0A6, Canada
[14]Department of Pathology and Laboratory Medicine, University of Pennsylvania, Philadelphia, PA 19104, USA
[15]Lead Contact
*Correspondence: etienne.simon-loriere@pasteur.fr (E.S.-L.), jonathan.ball@nottingham.ac.uk (J.K.B.)
http://dx.doi.org/10.1016/j.cell.2016.10.013

SUMMARY

The 2013–2016 outbreak of Ebola virus (EBOV) in West Africa was the largest recorded. It began following the cross-species transmission of EBOV from an animal reservoir, most likely bats, into humans, with phylogenetic analysis revealing the co-circulation of several viral lineages. We hypothesized that this prolonged human circulation led to genomic changes that increased viral transmissibility in humans. We generated a synthetic glycoprotein (GP) construct based on the earliest reported isolate and introduced amino acid substitutions that defined viral lineages. Mutant GPs were used to generate a panel of pseudoviruses, which were used to infect different human and bat cell lines. These data revealed that specific amino acid substitutions in the EBOV GP have increased tropism for human cells, while reducing tropism for bat cells. Such increased infectivity may have enhanced the ability of EBOV to transmit among humans and contributed to the wide geographic distribution of some viral lineages.

INTRODUCTION

Since its beginnings in December 2013, the West African outbreak of Ebola virus (EBOV; Makona variant) has resulted in more than 28,000 confirmed or suspected cases and more than 11,000 deaths (W.H.O., 2016). As with previous human outbreaks, the West African epidemic began following the successful cross-species transmission of EBOV from an animal reservoir into humans, with mounting evidence that a number of bat species are the likely natural reservoir and maintain the virus between human outbreaks (Leroy et al., 2005; Ogawa et al., 2015). The successful ongoing transmission of viruses within a new host species is often associated with the acquisition of host-adaptive mutations (Moncla et al., 2016; Pepin et al., 2010). Minor changes in the EBOV glycoprotein (GP) can impact its ability to mediate viral entry into cells from different mammalian species (Ng et al., 2015), such that it is clearly a major component of host specificity and viral fitness. Although the evolution of EBOV Makona during the West African outbreak was characterized by the emergence and spread of genetically distinct viral lineages (Carroll et al., 2015; Gire et al., 2014; Ladner et al., 2015; Quick et al., 2016; Simon-Loriere et al., 2015; Tong et al., 2015), it is unknown whether this prolonged human circulation enabled the virus to better adapt to exclusively human transmission. We speculated that a number of GP substitutions, including those at potential N-linked glycosylation sites and those within and around the mucin-like domain (Lee et al., 2008), could affect GP-mediated entry and, in turn, facilitate human adaptation.

RESULTS

To identify GP amino acid changes that may have increased viral transmissibility in humans, we compared 1,610 full-length genome sequences of EBOV Makona viruses from the West African outbreak of 2013–2016. These viruses were sampled from Guinea, Sierra Leone, Liberia, and Mali. Phylogenetic analysis of

This is an open access article under the CC BY-NC-ND license (http://creativecommons.org/licenses/by-nc-nd/4.0/).

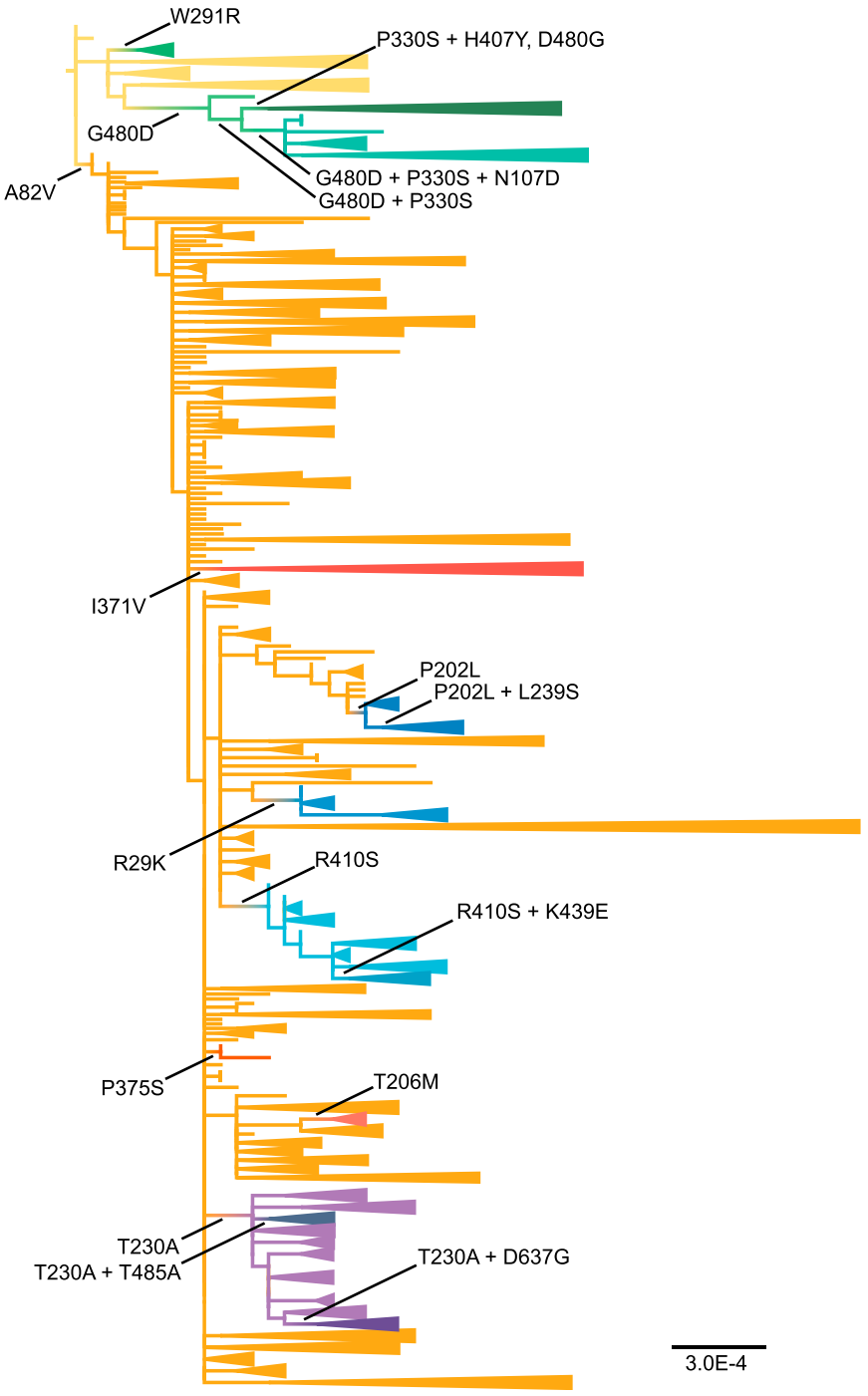

Figure 1. Schematic Maximum Likelihood Phylogenetic Tree of 1,610 Complete EBOV Makona Genomes

The tree is color coded according to lineage, and the lineage-defining amino acid substitutions in the viral GP studied here are marked. To enhance data display, monophyletic groups of sequences were collapsed, and the tree was vertically compressed in multiple sections. The tree was rooted using the earliest Kissidougou-C15 sequence, and all horizontal branch lengths are drawn to a scale of nucleotide substitutions per site. An expanded tree is presented in Data S1.

these sequences revealed the presence of two major lineages: lineage A, which only comprised sequences obtained from Guinea, including the earliest sampled viruses from the outbreak as a whole; and lineage B, which contained a much larger number of sequences (including those previously assigned to lineages SL1, SL2, and SL3 [Gire et al., 2014]) from all of the affected countries and hence has a far wider geographic distribution (Figure 1 and Data S1). Mapping all GP amino acid substitutions onto our whole-genome phylogeny revealed that lineages A and B are distinguished by a single Ala-Val amino acid substitution in the receptor binding domain (RBD) of GP at residue 82 (A82V; Figure 1). In addition, both lineages A and B contained a number of sub-lineages that were defined by additional amino acid substitutions elsewhere in the GP (Figure 1 and Data S1).

To determine whether these lineage-specific amino acid substitutions resulted in more efficient human cell infection, and hence increased fitness, we generated a panel of GP mutants based on the earliest sampled Makona isolate, Kissidougou-C15 (GenBank: KJ660346, sampled from Guinea in March 2014; Figure 2), and tested their ability to support entry into a range of human and bat cell lines using a lentiviral pseudotype assay (Urbanowicz et al., 2016). Although variants from both lineages A and B reached higher infectivity in human cells than Kissidougou-C15 (Figure 3), the A82V change appears to have set the GP on separate evolutionary pathways, as we observed distinct sets of additional amino acid changes in each lineage that increased entry efficacy in human cells. However, despite the evolutionary diversification that was apparent in both lineages, the V82 background (lineage B) appeared conducive to reaching higher infectivity than viruses with A82 (lineage A; Figure 3).

The A82V substitution (variant B1) alone resulted in an almost 2-fold increase in infectivity in human cells compared to the reference Kissidougou-C15 strain (Figure 3; $p < 0.01$). Other amino acid changes further increased the effect of A82V. For example, R29K (variant B7), which falls within the GP signal peptide, resulted in a major increase in entry efficacy. Similarly, substitutions T206M (variant B12) and T230A (variant B13) in the GP glycan cap, which resulted in a loss of conserved

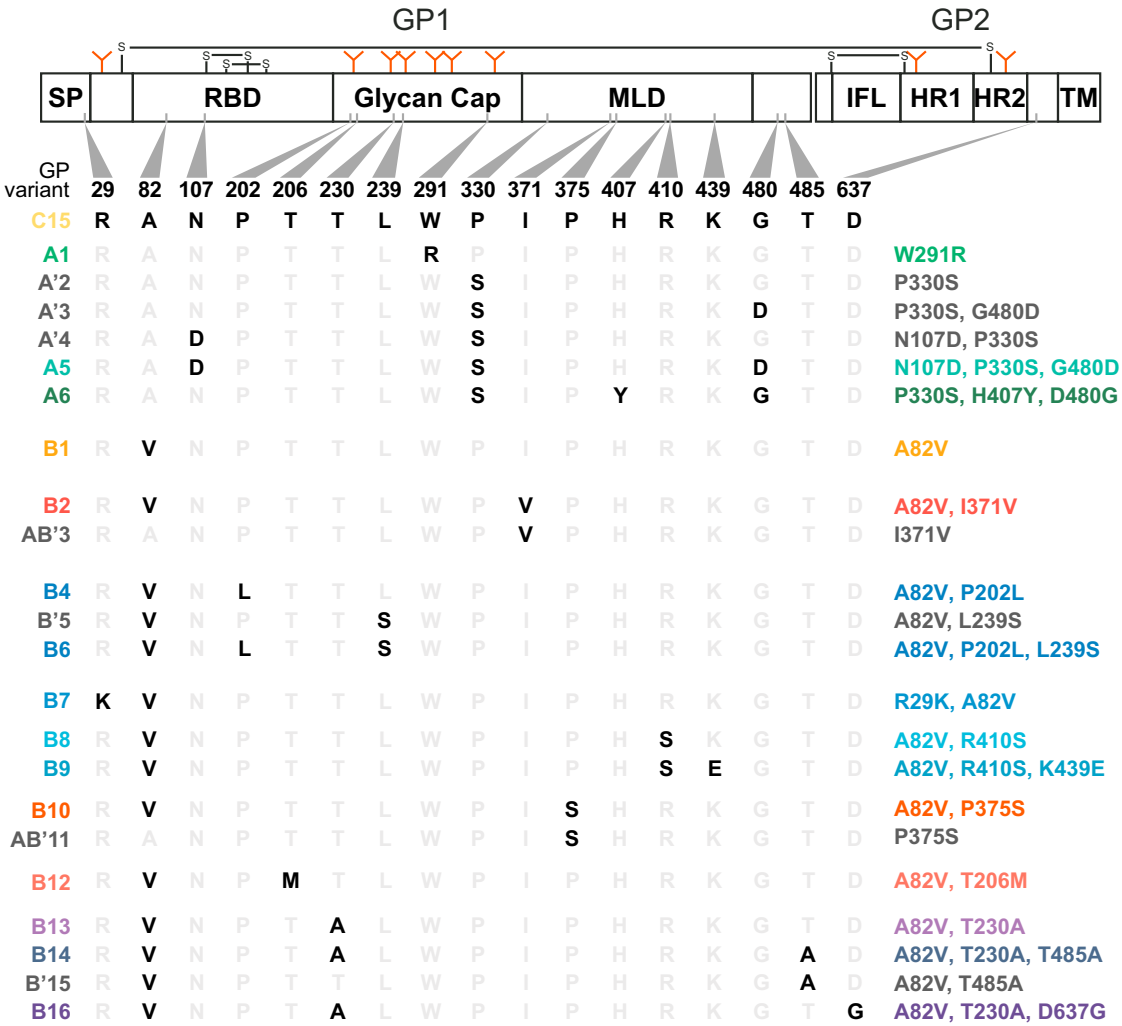

Figure 2. Schematic of the 17 Lineage-Defining Amino Acid Combinations in the EBOV GP

Amino acid changes identified on the EBOV Makona phylogeny presented in Figure 1 are shown in black. The GP scheme is drawn to scale. SP: signal peptide; RBD: receptor binding domain; MLD: mucin-like domain; IFL: internal fusion loop; HR: heptad repeat; TM: transmembrane domain. Also indicated to the left of the alignment is the assigned variant name, where A and B denote lineage A (82A) and B (82V) backgrounds, respectively. Prime (′) indicates variants not sampled during the outbreak and AB′ has been used to identify variants generated to investigate the impact of 82A background on lineage-B-defined substitutions. On the right-hand side, the specific combination of amino acid substitutions compared to the reference strain. Colors relate to the lineages identified in Figure 1.

N-glycosylation branching at N204 and N228, respectively, strongly increased GP entry in human cells. Subsequent substitutions in the T230A cluster of EBOV sequences, such as T485A (variant B14) in the mucin-like domain of GP or D637G at the end of GP2 (variant B16), did not appear to modulate viral entry further. Within the more geographically restricted lineage A, variant A1, containing a single W291R substitution in the glycan cap, resulted in a marked increase in entry efficacy in HuH7 and BEAS-2B cells (Figure 3; $p < 0.01$).

These data also revealed the importance of epistatic interactions to viral adaptation. In lineage A, we observed strong positive epistasis involving residue 330. Specifically, following an initial G480D change, a P330S substitution occurred with either N107D (variant A6) or H407Y after a reversion of G480D (variant A5; Figure 1). Strikingly, the co-occurrence of P330S with G480D evolved independently in lineage B (Data S1), compatible with the idea that, in combination, these mutants increase fitness. Indeed, in our HuH7 entry assay, mutants A5 and A6 were significantly more entry efficient than the reference Kissidougou-C15 strain (Figure 3; $p < 0.05$ and $p < 0.01$, respectively). In contrast, variants with the P330S substitution alone (mutant A′2), or in combination with either G480D (mutant A′3) or N107D (mutant A′4), were all less infectious than the reference sequence in HuH7 cells ($p < 0.05$); none of these changes were sampled during the outbreak.

The impact of epistasis can also be seen within lineage B involving glycan cap domain residues P202L and L239S. While the initial P202L substitution (variant B4) decreased infectivity in HuH7 cells compared to the A82V mutant, the subsequent emergence of L239S (variant B6), which occurred in two different

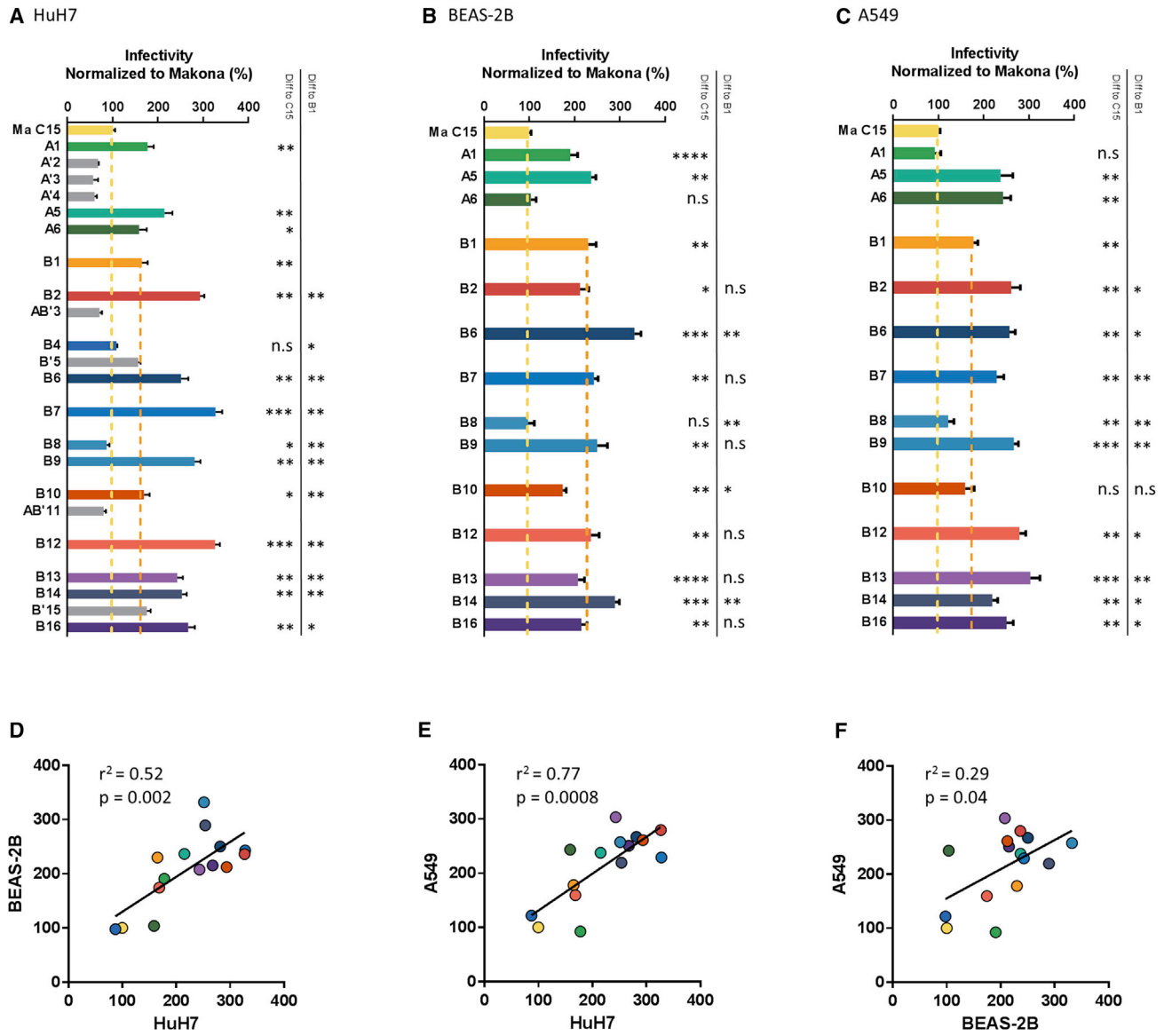

Figure 3. Differential Infectivity of Pseudoviruses Supplemented with EBOV Makona GP Mutants in Human Cells

(A–C) Relative infectivity of each glycoprotein was expressed as a proportion (%) of that observed for the Kissidougou-C15 strain in HuH7 (A), BEAS-2B (B), and A549 (C) cells. Histogram bar colors correspond to the lineage color-coding shown in Figure 1, with gray bars indicating variants not sampled during the outbreak. These data are the means ± 1 SD of either two (non-sampled variants) or three (sampled variants) independent experiments, each performed in triplicate. Differences in the mean infectivity of each outbreak-associated mutant compared to the Kissidougou-C15 EBOV strain and the lineage B viruses to the A82V mutant were assessed using repeated-measures one-way ANOVA with Dunnett's multiple comparison test and indicated in the table inset; *$p < 0.05$; **$p < 0.01$; ***$p < 0.001$; n.s., not significant.

(D–F) Plots of normalized infectivity for the three human cell lines and correlations were calculated using Pearson's correlation test. See also Figure S2.

branches within this cluster (Data S1), resulted in significantly higher infectivity than the A82V change alone in all human cell lines tested ($p < 0.01$). Importantly, the L239S substitution alone, which was not observed during the outbreak, did not result in increased entry (variant B′5; Figure 3). This again suggests that fitness increases result from epistatic interactions.

GP residue 82 was also seemingly involved in epistatic interactions. For example, the I371V change (variant B2), which defines a large cluster of sequences from Sierra Leone (Data S1), increased entry efficacy up to 2-fold in the 82V background (lineage B). However, in the context of the 82A background that defines lineage A, I371V (variant AB′3) decreased HuH7 cell infectivity ($p < 0.001$). The AB′3 variant was not sampled during the outbreak. Conversely, the presence of P375S, in association with 82A, increased infectivity (variant AB′11) but decreased infectivity in the presence of 82V (variant B10; Figure 3).

While the majority of amino acid substitutions observed in the outbreak improved human cell entry, some changes in lineage B,

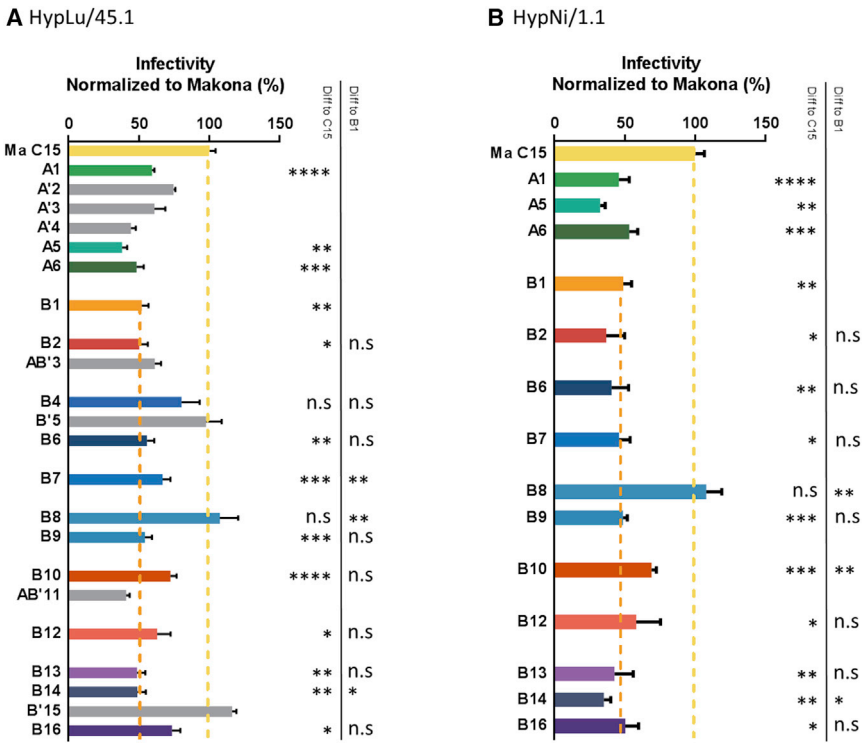

Figure 4. Differential Infectivity of Pseudoviruses Supplemented with EBOV Glycoprotein Mutants in Different Bat Cell Lines

(A and B) Relative infectivity of each glycoprotein was expressed as a proportion (%) of that observed for the Kissidougou-C15 strain in HypLu/45.1 (A) and HypNi/1.1(B) cells. Histogram bar colors correspond to the lineage color coding shown in Figure 1, with gray bars indicating variants not sampled during the outbreak. These data are the means ± 1 SD of either two (non-sampled variants) or three (sampled variants) independent experiments, each performed in triplicate. Differences in the mean infectivity of each outbreak-associated mutant compared to the Kissidougou-C15 EBOV strain and the lineage B viruses to the A82V mutant were assessed using repeated-measures one-way ANOVA with Dunnett's multiple comparison test and indicated in the table inset; *$p < 0.05$; **$p < 0.01$; ***$p < 0.001$; n.s., not significant. See also Figure S1.

including R410S (variant B8), resulted in reduced fitness. Notably, a subset of viruses in this cluster acquired an additional K439E change (variant B9) that enhanced entry efficacy 3-fold ($p < 0.01$) in HuH7 cells. Interestingly, a set of lineage B viruses with R410S and K439E were sampled in a community of fishermen in Sierra Leone, characterized by an unusually severe disease presentation (Capobianchi et al., 2015). Finally, it is important to note that pseudovirus entry in one human cell line correlated well with the infectivity observed in the other human lines tested (Figures 3D–3F), indicating that the effect was independent of the anatomical site from where the cells were derived.

Having seen evidence of adaptation to human cells, we next determined whether EBOV evolution during the outbreak impacted the entry into liver and kidney cell lines derived from *Hypsignathus monstrosus*, one of the putative fruit bat hosts. The most striking feature of this analysis was the general reversal in infectivity compared to human cells (Figure 4); indeed, there was a statistically significant negative correlation between infectivity in *H. monstrosus* compared to human cell lines (Figure 5). Obvious reversals in phenotype were apparent for individual mutants. For example, the lineage B variant R410S (variant B8), which resulted in low entry efficacy in human cells, was highly efficient in infecting *H. monstrosus* cells. In contrast, the additional K439E substitution (variant B9), which enhanced infectivity in human cells, abolished this effect ($p < 0.05$; Figure 4). This pattern of decreased infectivity in fruit bat cells concomitant with GP evolution was also observed for kidney cells derived from *Epomops buettikoferi* (Figure S1A) and *Rousettus aegyptiacus* bats (Figure S1B), although the strength of the effect, and hence the correlations of infectivity in human cells compared to these alternative fruit bat cells, were less pronounced (Figure S2). Finally, we assessed EBOV-GP-mediated entry in cell lines derived from the insectivorous bats *Hipposideros abae* and *Myotis daubentonii*. Neither of these could be infected by EBOV GP pseudoviruses but were permissive for entry by PVs supplemented with control VSV G protein (data not shown).

DISCUSSION

Although the genome-scale evolution of EBOV during the West African outbreak has been described in detail (Carroll et al., 2015; Gire et al., 2014; Ladner et al., 2015; Quick et al., 2016; Simon-Loriere et al., 2015; Tong et al., 2015), little is known about whether the virus also experienced heritable changes in phenotype during the outbreak, including adaptation to exclusively human transmission. As selectively advantageous mutations that spread through the viral population will fall on deeper branches on the phylogeny, we identified a number of lineage-defining GP amino acid substitutions and, using a pseudotype entry assay, showed that many of these conferred increased human cell entry. Hence, these data strongly suggest that a number of specific amino acid substitutions in EBOV, particularly although not exclusively A82V, increased tropism for human cells and facilitated adaptive evolution. Interestingly, the reported increase in overall viremia in the Conakry (Guinea) area during the summer of 2014 (Faye et al., 2015) is coincident with the introduction of lineage B variants from Sierra Leone. An accompanying manuscript from Diehl and colleagues in this issue of *Cell* independently shows that A82V increased viral infectivity in a variety of human primary cells and continuous cell lines, supporting the hypothesis that A82V is a fitness adaptation (Diehl et al., 2016).

Residue 82 lies in a short α-helix (termed α1) of the RBD, which is involved in binding the filovirus receptor protein Niemann-Pick

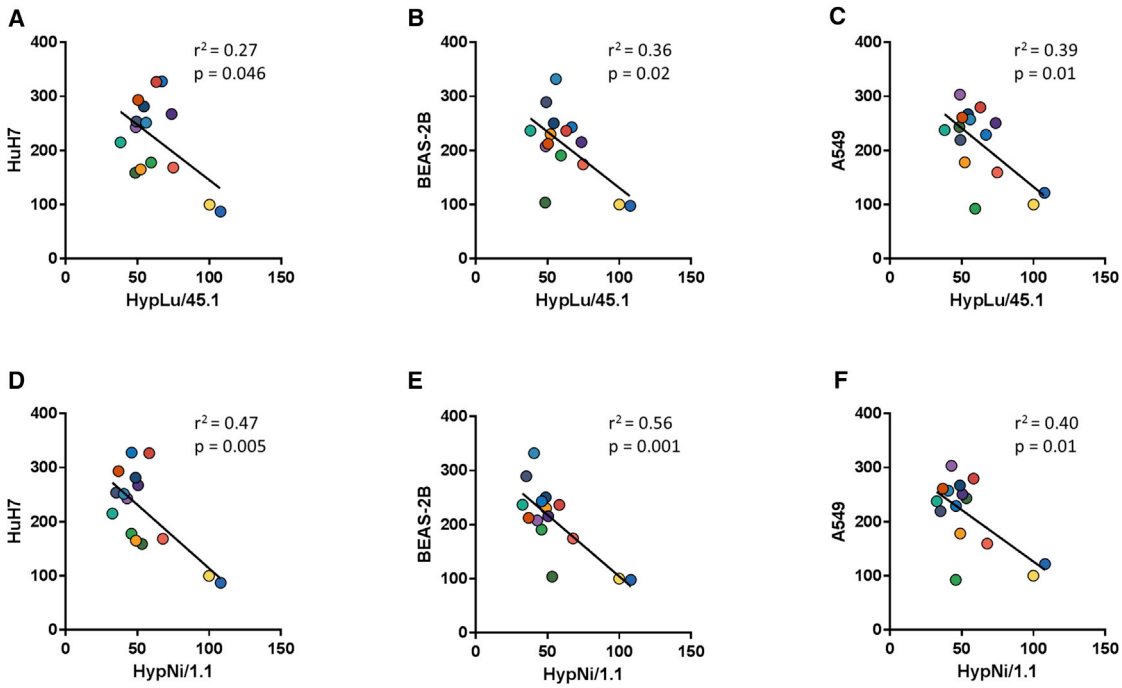

Figure 5. Negative Correlation of GP Mutant Infectivity between *Hypsignathus Monstrosus* Cells and Human Cells

(A–F) Normalized infectivity data for each GP mutant were plotted for HypLu/45.1 cells versus HuH7 (A), BEAS-2B (B), and A549 (C) and HypNi/1.1 cells versus HuH7 (D), BEAS-2B (E), and A549 (F). Infectivity data are the same as that shown in Figures 3 and 4. Correlations were determined using Pearson's correlation test.

C1 (NPC1). In the helix, residue 82 points toward the hydrophobic core of GP in the face opposing the one contacted by NPC1. The crystal structure of the complex (Wang et al., 2016) shows that the interaction with the receptor results in displacement (gliding) of the helix along the hydrophobic core of the GP (Figure 6), implying that the nature of the side chain at position 82 will affect this gliding. Homology modeling (data not shown) shows that the presence of valine instead of alanine makes the α1 helix slightly protrude outward to accommodate the two extra methyl groups of its side chain. Although the residues in bat NPC1 that are directly contacted by the GP α1 helix are conserved with respect to human NPC1, some changes fall nearby, for instance, residue NPC1 127 (labeled in green in Figure 6), which is a charged lysine in human NPC1 and a hydrophobic isoleucine in bats. This could lead to a more favorable overall interaction with human versus bat NPC1. Indeed, single substitutions in the two protruding loops of NPC1 that contact the GP were shown to restrict host susceptibility to EBOV (Ng et al., 2015). The reduction of infectivity in bat cells associated with the lineage-defining A82V substitution further highlights the key role played by amino acid changes in and around the α1 helix of the GP in modulating EBOV entry in different mammalian hosts (Martinez et al., 2013). In addition, because there is a rearrangement of the GP in the region of the α1 helix upon receptor binding, it is possible that the A82V change may also affect the dynamics of the conformational changes that occur during the entry process. Indeed, a number of epistatic changes, for example, I371V and P375S, were associated with residue 82, and these observations hint at functional interactions between the mucin-like domain, cleaved during GP priming, and the receptor-binding domain, which must be uncovered after cleavage for NPC1 binding to take place (Figure 6A).

In addition to A82V, a number of additional amino acid changes that arose during the outbreak also conferred increased efficiency for human cell entry. One of these—R29K (variant B7) —was located in the signal peptide, mutations in which have previously been associated with changes in glycosylation and the enhancement of infectivity (Marzi et al., 2006). Similarly, mutations that resulted in the loss of conserved N-glycosylation sites (T206M in variant B12 and T230A in variant B13, affecting N-glycosylation on N204 and N228) strongly increased GP entry into human cells. Removal of N-glycosylation sites has been shown to enhance viral entry in vitro, although leaving the GP more susceptible to neutralization (Lennemann et al., 2014). Coincidently, amino acid substitutions that occurred following the emergence of the T230A change (such as T485A; variant B14 and D637G; variant B16), while not impacting cell entry, may have been involved in immune escape. For example, the threonine at residue 485 is a key determinant for binding by the highly neutralizing antibody 14G7, in which any amino acid aside from serine fully abolishes the interaction (Olal et al., 2012). Correspondingly, T485A also had no effect on GP entry efficacy in the context of A230T (variant B′15; Figure 3). Similarly, the R410S substitution, which lies in a B cell epitope that is a dominant target for humoral responses (Capobianchi et al., 2015) and does not improve viral entry, might also have been favored by immune selection. Antibody protection underpins a number of emerging vaccines and therapies, so it will be important for

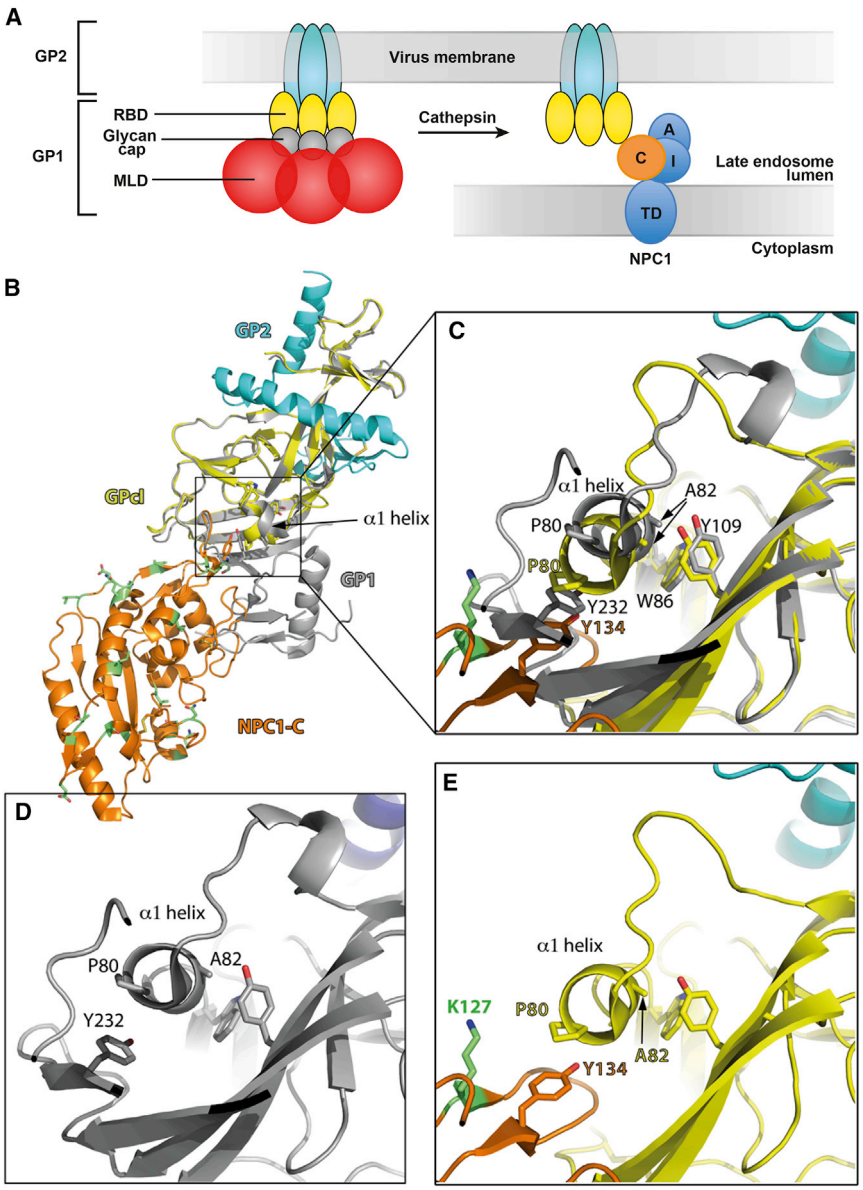

Figure 6. Residue 82 in the GPcl/NPC1-C Complex

(A) Cartoon showing the organization of the GP complex as anchored in the viral membrane, colored according to domains as labeled (left). The right panel shows the cleaved GP (GPcl), i.e., what remains on the viral membrane after cathepsin cleavage in the endosome, which eliminates the glycan cap and the mucin-like domain (MLD) from the GP trimer. The endosomal membrane and the multiple transmembrane spanning protein NPC1 (Gong et al., 2016) are also shown, with domain C, which is bound by cleaved GP, in orange, contacted by the RBD of GP.

(B) Crystal structure of NPC1-C domain in complex with GPcl (PDB 5F1B [Wang et al., 2016]). NPC1-C is in orange, and residues that are different in bat NPC1-C displayed in green and with sticks. GPcl is shown in yellow, with the GP2 moiety in cyan (as in the cartoon in A). Overlaid is the structure of the GP complex in its pre-fusion form (gray, PDB 3SCY [Lee et al., 2008]), which lacks the MLD but still contains the glycan cap. The side chains of GP1 Y232 and NPC1-C Y134 are shown in sticks. The α1 helix, which moves upon complex formation, is indicated.

(C) Zoom of the region framed in (B), rotated to better display the interactions. The ring of P80, the first residue on the α1 helix, packs against the phenol ring of Y232 within GP1 prior to cathepsin cleavage. Removal of the 191–503 region after cathepsin cleavage frees the α1 helix to interact with NPC1-C, where Y134 takes the same place. The helix packs against the side chains of W86 and Y109, which remain relatively unchanged, while A82 glides downward, accompanying the movement of P80 to maintain the interaction with NPC1-C Y134 in the complex. Because the environment is different in bat NPC1, where residue 127 (labeled in green in (B)) changes from a charged lysine to a hydrophobic isoleucine, our data point to a more favorable interaction with the human NPC1 by acquiring a valine at position 82.

(D and E) Same as (C) but showing, for clarity, only the individual structures in the same orientation.

future studies to define the impact of GP evolution on antibody-mediated immunity.

There is conflicting evidence on whether EBOV is restricted to fruit bats (Leroy et al., 2005; Ogawa et al., 2015; Pourrut et al., 2007; Swanepoel et al., 1996) or if it is also present in insectivorous bat species (Han et al., 2016; Leendertz et al., 2016; Pourrut et al., 2009; Swanepoel et al., 1996). For example, Marí Saéz et al. (2014) suggested that the 2013–2016 outbreak might have originated from a spill-over involving the insectivorous bat species *Mops condylurus*, although no EBOV-positive wildlife species have been documented in the area to date. Our finding that *Hipposideros abae* and *Myotis daubentonii* insectivorous bat cell lines were non-permissive for all the EBOV GP pseudoviruses lends credence to the hypothesis that fruit bats, rather than insectivorous bats, are the likely natural reservoir for EBOV.

Overall, these data provide strong evidence that specific amino acid substitutions in the EBOV glycoprotein that arose during the 2013–2016 outbreak affect entry and increase tropism for human cells while simultaneously reducing tropism for fruit bat cells. These changes, involving various modifications in glycosylation, as well as subtle structural changes in the receptor binding α1 helix, may therefore have enhanced the ability of EBOV to transmit among humans, particularly those viruses of lineage B that spread to multiple countries throughout the affected region. Although some studies have suggested that the EBOV Makona genome carries signatures of positive selection compatible with adaptive evolution (Liu et al., 2015), others have argued against this process (Azarian et al., 2015; Hoenen et al., 2015; Olabode et al., 2015). Critically, however, all these studies have relied exclusively on genome sequence

comparisons without access to the types of experimental data generated here that clearly demonstrate changes in viral phenotype. In addition, some comparative studies have ruled out adaptive evolution by considering the EBOV phylogeny as a whole, thereby failing to distinguish short-term evolution during human outbreaks such as that in West Africa from the far longer evolutionary history in the reservoir species (Olabode et al., 2015).

Despite the experimental data provided here, it is impossible to clearly establish whether the adaptive mutations observed were in part responsible for the extended duration of the 2013–2016 epidemic. Indeed, it seems likely that the prolonged nature of the outbreak in West Africa was primarily due to epidemiological factors, such as an increased circulation in urban areas that in turn led to larger chains of transmission. It is also important to recall that EBOV has crossed the species barrier from its reservoir hosts to humans on multiple occasions since the first report of EBOV in 1976. Hence, most, if not all, animal variants of EBOV have the ability to effectively transmit among humans such that host adaptation is not a pre-requisite for future outbreaks. Similarly, it is impossible on current data to determine whether and how the amino acid substitutions observed in the EBOV Makona genome might have impacted pathogen virulence. However, because there is a strong positive correlation between EBOV viremia and mortality (Faye et al., 2015; Fitzpatrick et al., 2015; Schieffelin et al., 2014), increased transmissibility could conceivably result in viruses of enhanced virulence, although this clearly needs to be addressed with additional studies.

STAR★METHODS

Detailed methods are provided in the online version of this paper and include the following:

- KEY RESOURCES TABLE
- CONTACT FOR REAGENT AND RESOURCE SHARING
- EXPERIMENTAL MODEL AND SUBJECT DETAILS
  - Cells
- METHOD DETAILS
  - Phylogenetic analysis
  - Construction of Ebola virus glycoprotein mutant panel
  - Transfection
  - Pseudovirus infection assays
  - Modeling
- QUANTIFICATION AND STATISTICAL ANALYSIS

SUPPLEMENTAL INFORMATION

Supplemental Information includes two figures, one table, and one dataset and can be found with this article online at http://dx.doi.org/10.1016/j.cell.2016.10.013.

AUTHOR CONTRIBUTIONS

Conceptualization, R.A.U., E.S.-L., and J.K.B.; Formal Analysis, R.A.U., E.S.-L., F.A.R. and J.K.B.; Investigation, R.A.U., C.P.M., F.A.R., E.C.H., and E.S.-L.; Resources, A.S, A.A.S., G.K., and M.A.M.; Writing – Original Draft, E.S.-L., E.C.H., and J.K.B.; Writing – Review and Editing, E.S.-L., E.C.H., J.K.B., R.A.U., F.A.R., G.K, C.P.M., and M.A.M.; Visualization, R.A.U., J.K.B., F.A.R., and E.S.-L.; Supervision, J.K.B. and E.C.H.; Funding Acquisition, E.S.-L., and J.K.B.

ACKNOWLEDGMENTS

This study was supported by funding from the Medical Research Council (G0801169), the Biotechnology and Biological Sciences Research Council (BB/M018636/1), the French Government's Investissement d'Avenir program, Laboratoire d'Excellence "Integrative Biology of Emerging Infectious Diseases" (grant n°ANR-10-LABX-62-IBEID), the Institut Pasteur Ebola Task Force, and the University of Nottingham Faculty of Medicine and Health Sciences International Research Collaboration Fund. E.C.H. is supported by an NHMRC Australia fellowship (AF30). Bat cells were generated within the framework of EU-FP7 ANTIGONE (no. 278976) and the EBOKON project supported by the Federal Ministry of Education and Research (BMBF). The authors would like to thank Prof. Greg Towers of University College London for discussions about host lentiviral restriction factors and Andrew Rambaut of University of Edinburgh for the sequence alignment dataset (see Key Resources Table).

Received: August 12, 2016
Revised: September 23, 2016
Accepted: October 6, 2016
Published: November 3, 2016

REFERENCES

Anisimova, M., and Gascuel, O. (2006). Approximate likelihood-ratio test for branches: A fast, accurate, and powerful alternative. Syst. Biol. *55*, 539–552.

Azarian, T., Lo Presti, A., Giovanetti, M., Cella, E., Rife, B., Lai, A., Zehender, G., Ciccozzi, M., and Salemi, M. (2015). Impact of spatial dispersion, evolution, and selection on Ebola Zaire Virus epidemic waves. Sci. Rep. *5*, 10170.

Besnier, C., Ylinen, L., Strange, B., Lister, A., Takeuchi, Y., Goff, S.P., and Towers, G.J. (2003). Characterization of murine leukemia virus restriction in mammals. J. Virol. *77*, 13403–13406.

Capobianchi, M.R., Gruber, C.E., Carletti, F., Meschi, S., Castilletti, C., Vairo, F., Biava, M., Minosse, C., Strada, G., Portella, G., et al. (2015). Molecular signature of the ebola virus associated with the fishermen community outbreak in Aberdeen, Sierra Leone, in February 2015. Genome Announc. Published online September 24, 2015. https://dx.doi.org/10.1128/genomeA.01093-15.

Carroll, M.W., Matthews, D.A., Hiscox, J.A., Elmore, M.J., Pollakis, G., Rambaut, A., Hewson, R., Garcia-Dorival, I., Bore, J.A., Koundouno, R., et al. (2015). Temporal and spatial analysis of the 2014-2015 Ebola virus outbreak in West Africa. Nature *524*, 97–101.

Diehl, W.E., Lin, A.E., Grubaugh, N.D., Carvalho, L.M., Kyusik, K., Kyawe, P.P., McCauley, S.M., Donnard, E., Kucukural, A., McDonel, P., et al. (2016). Ebola virus glycoprotein with increased infectivity dominated the 2013-2016 epidemic. Cell *167*, this issue, 1088–1098.

Faye, O., Andronico, A., Faye, O., Salje, H., Boëlle, P.Y., Magassouba, N., Bah, E.I., Koivogui, L., Diallo, B., Diallo, A.A., et al. (2015). Use of Viremia to Evaluate the Baseline Case Fatality Ratio of Ebola Virus Disease and Inform Treatment Studies: A Retrospective Cohort Study. PLoS Med. *12*, e1001908.

Fitzpatrick, G., Vogt, F., Moi Gbabai, O.B., Decroo, T., Keane, M., De Clerck, H., Grolla, A., Brechard, R., Stinson, K., and Van Herp, M. (2015). The Contribution of Ebola Viral Load at Admission and Other Patient Characteristics to Mortality in a Medecins Sans Frontieres Ebola Case Management Centre, Kailahun, Sierra Leone, June-October 2014. J. Infect. Dis. *212*, 1752–1758.

Gire, S.K., Goba, A., Andersen, K.G., Sealfon, R.S., Park, D.J., Kanneh, L., Jalloh, S., Momoh, M., Fullah, M., Dudas, G., et al. (2014). Genomic surveillance elucidates Ebola virus origin and transmission during the 2014 outbreak. Science *345*, 1369–1372.

Gong, X., Qian, H., Zhou, X., Wu, J., Wan, T., Cao, P., Huang, W., Zhao, X., Wang, X., Wang, P., et al. (2016). Structural Insights into the Niemann-Pick C1 (NPC1)-Mediated Cholesterol Transfer and Ebola Infection. Cell *165*, 1467–1478.

Guindon, S., Dufayard, J.F., Lefort, V., Anisimova, M., Hordijk, W., and Gascuel, O. (2010). New algorithms and methods to estimate maximum-likelihood phylogenies: assessing the performance of PhyML 3.0. Syst. Biol. *59*, 307–321.

Han, B.A., Schmidt, J.P., Alexander, L.W., Bowden, S.E., Hayman, D.T., and Drake, J.M. (2016). Undiscovered Bat Hosts of Filoviruses. PLoS Negl. Trop. Dis. *10*, e0004815.

Herrera, C., Klasse, P.J., Michael, E., Kake, S., Barnes, K., Kibler, C.W., Campbell-Gardener, L., Si, Z., Sodroski, J., Moore, J.P., and Beddows, S. (2005). The impact of envelope glycoprotein cleavage on the antigenicity, infectivity, and neutralization sensitivity of Env-pseudotyped human immunodeficiency virus type 1 particles. Virology *338*, 154–172.

Hoenen, T., Safronetz, D., Groseth, A., Wollenberg, K.R., Koita, O.A., Diarra, B., Fall, I.S., Haidara, F.C., Diallo, F., Sanogo, M., et al. (2015). Virology. Mutation rate and genotype variation of Ebola virus from Mali case sequences. Science *348*, 117–119.

Kuhl, A., Hoffmann, M., Muller, M.A., Munster, V.J., Gnirss, K., Kiene, M., Tsegaye, T.S., Behrens, G., Herrler, G., Feldmann, H., et al. (2011). Comparative analysis of Ebola virus glycoprotein interactions with human and bat cells. J. Infect. Dis. *204* (*Suppl 3*), S840–S849.

Ladner, J.T., Wiley, M.R., Mate, S., Dudas, G., Prieto, K., Lovett, S., Nagle, E.R., Beitzel, B., Gilbert, M.L., Fakoli, L., et al. (2015). Evolution and Spread of Ebola Virus in Liberia, 2014-2015. Cell Host Microbe *18*, 659–669.

Lee, J.E., Fusco, M.L., Hessell, A.J., Oswald, W.B., Burton, D.R., and Saphire, E.O. (2008). Structure of the Ebola virus glycoprotein bound to an antibody from a human survivor. Nature *454*, 177–182.

Leendertz, S.A., Gogarten, J.F., Düx, A., Calvignac-Spencer, S., and Leendertz, F.H. (2016). Assessing the Evidence Supporting Fruit Bats as the Primary Reservoirs for Ebola Viruses. EcoHealth *13*, 18–25.

Lennemann, N.J., Rhein, B.A., Ndungo, E., Chandran, K., Qiu, X., and Maury, W. (2014). Comprehensive functional analysis of N-linked glycans on Ebola virus GP1. MBio *5*, e00862–e13.

Leroy, E.M., Kumulungui, B., Pourrut, X., Rouquet, P., Hassanin, A., Yaba, P., Délicat, A., Paweska, J.T., Gonzalez, J.P., and Swanepoel, R. (2005). Fruit bats as reservoirs of Ebola virus. Nature *438*, 575–576.

Liu, S.Q., Deng, C.L., Yuan, Z.M., Rayner, S., and Zhang, B. (2015). Identifying the pattern of molecular evolution for Zaire ebolavirus in the 2014 outbreak in West Africa. Infect. Genet. Evol. *32*, 51–59.

Marí Saéz, A., Weiss, S., Nowak, K., Lapeyre, V., Zimmermann, F., Düx, A., Kühl, H.S., Kaba, M., Regnaut, S., Merkel, K., et al. (2014). Investigating the zoonotic origin of the West African Ebola epidemic. EMBO Mol. Med. *7*, 17–23.

Martinez, O., Ndungo, E., Tantral, L., Miller, E.H., Leung, L.W., Chandran, K., and Basler, C.F. (2013). A mutation in the Ebola virus envelope glycoprotein restricts viral entry in a host species- and cell-type-specific manner. J. Virol. *87*, 3324–3334.

Marzi, A., Akhavan, A., Simmons, G., Gramberg, T., Hofmann, H., Bates, P., Lingappa, V.R., and Pöhlmann, S. (2006). The signal peptide of the ebolavirus glycoprotein influences interaction with the cellular lectins DC-SIGN and DC-SIGNR. J. Virol. *80*, 6305–6317.

Mohan, G.S., Ye, L., Li, W., Monteiro, A., Lin, X., Sapkota, B., Pollack, B.P., Compans, R.W., and Yang, C. (2015). Less is more: Ebola virus surface glycoprotein expression levels regulate virus production and infectivity. J. Virol. *89*, 1205–1217.

Moncla, L.H., Zhong, G., Nelson, C.W., Dinis, J.M., Mutschler, J., Hughes, A.L., Watanabe, T., Kawaoka, Y., and Friedrich, T.C. (2016). Selective Bottlenecks Shape Evolutionary Pathways Taken during Mammalian Adaptation of a 1918-like Avian Influenza Virus. Cell Host Microbe *19*, 169–180.

Nakabayashi, H., Taketa, K., Miyano, K., Yamane, T., and Sato, J. (1982). Growth of human hepatoma cells lines with differentiated functions in chemically defined medium. Cancer Res. *42*, 3858–3863.

Ng, M., Ndungo, E., Kaczmarek, M.E., Herbert, A.S., Binger, T., Kuehne, A.I., Jangra, R.K., Hawkins, J.A., Gifford, R.J., Biswas, R., et al. (2015). Filovirus receptor NPC1 contributes to species-specific patterns of ebolavirus susceptibility in bats. eLife *4*, e11785.

Ogawa, H., Miyamoto, H., Nakayama, E., Yoshida, R., Nakamura, I., Sawa, H., Ishii, A., Thomas, Y., Nakagawa, E., Matsuno, K., et al. (2015). Seroepidemiological Prevalence of Multiple Species of Filoviruses in Fruit Bats (Eidolon helvum) Migrating in Africa. J. Infect. Dis. *212* (*Suppl 2*), S101–S108.

Olabode, A.S., Jiang, X., Robertson, D.L., and Lovell, S.C. (2015). Ebolavirus is evolving but not changing: No evidence for functional change in EBOV from 1976 to the 2014 outbreak. Virology *482*, 202–207.

Olal, D., Kuehne, A.I., Bale, S., Halfmann, P., Hashiguchi, T., Fusco, M.L., Lee, J.E., King, L.B., Kawaoka, Y., Dye, J.M., Jr., and Saphire, E.O. (2012). Structure of an antibody in complex with its mucin domain linear epitope that is protective against Ebola virus. J. Virol. *86*, 2809–2816.

Pepin, K.M., Lass, S., Pulliam, J.R., Read, A.F., and Lloyd-Smith, J.O. (2010). Identifying genetic markers of adaptation for surveillance of viral host jumps. Nat. Rev. Microbiol. *8*, 802–813.

Pourrut, X., Délicat, A., Rollin, P.E., Ksiazek, T.G., Gonzalez, J.P., and Leroy, E.M. (2007). Spatial and temporal patterns of Zaire ebolavirus antibody prevalence in the possible reservoir bat species. J. Infect. Dis. *196* (*Suppl 2*), S176–S183.

Pourrut, X., Souris, M., Towner, J.S., Rollin, P.E., Nichol, S.T., Gonzalez, J.P., and Leroy, E. (2009). Large serological survey showing cocirculation of Ebola and Marburg viruses in Gabonese bat populations, and a high seroprevalence of both viruses in Rousettus aegyptiacus. BMC Infect. Dis. *9*, 159.

Quick, J., Loman, N.J., Duraffour, S., Simpson, J.T., Severi, E., Cowley, L., Bore, J.A., Koundouno, R., Dudas, G., Mikhail, A., et al. (2016). Real-time, portable genome sequencing for Ebola surveillance. Nature *530*, 228–232.

Reddel, R.R., Yang, K., Rhim, J.S., Brash, D., Su, R.T., Lechner, J.F., Gerwin, B.I., Harris, C.C., and Amstad, P. December 1989. Immortalized human bronchial epithelial mesothelial cell lines. U.S. patent US4885238 A.

Schieffelin, J.S., Shaffer, J.G., Goba, A., Gbakie, M., Gire, S.K., Colubri, A., Sealfon, R.S., Kanneh, L., Moigboi, A., Momoh, M., et al.; KGH Lassa Fever Program; Viral Hemorrhagic Fever Consortium; WHO Clinical Response Team (2014). Clinical illness and outcomes in patients with Ebola in Sierra Leone. N. Engl. J. Med. *371*, 2092–2100.

Simon-Loriere, E., Faye, O., Faye, O., Koivogui, L., Magassouba, N., Keita, S., Thiberge, J.M., Diancourt, L., Bouchier, C., Vandenbogaert, M., et al. (2015). Distinct lineages of Ebola virus in Guinea during the 2014 West African epidemic. Nature *524*, 102–104.

Smith, B.T. (1977). Cell line A549: a model system for the study of alveolar type II cell function. Am. Rev. Respir. Dis. *115*, 285–293.

Swanepoel, R., Leman, P.A., Burt, F.J., Zachariades, N.A., Braack, L.E., Ksiazek, T.G., Rollin, P.E., Zaki, S.R., and Peters, C.J. (1996). Experimental inoculation of plants and animals with Ebola virus. Emerg. Infect. Dis. *2*, 321–325.

Tong, Y.G., Shi, W.F., Di, L., Qian, J., Liang, L., Bo, X.C., Liu, J., Ren, H.G., Fan, H., Ni, M., et al. (2015). Genetic diversity and evolutionary dynamics of Ebola virus in Sierra Leone. Nature *524*, 93–96.

Urbanowicz, R.A., McClure, C.P., King, B., Mason, C.P., Ball, J.K., and Tarr, A.W. (2016). Novel functional hepatitis C virus glycoprotein isolates identified using an optimized viral pseudotype entry assay. J. Gen. Virol. *97*, 2265–2279.

Wang, H., Shi, Y., Song, J., Qi, J., Lu, G., Yan, J., and Gao, G.F. (2016). Ebola Viral Glycoprotein Bound to Its Endosomal Receptor Niemann-Pick C1. Cell *164*, 258–268.

W.H.O. (2016). Ebola Situation Report, W.H. Organisation, ed.

Yap, M.W., Colbeck, E., Ellis, S.A., and Stoye, J.P. (2014). Evolution of the retroviral restriction gene Fv1: inhibition of non-MLV retroviruses. PLoS Pathog. *10*, e1003968.

STAR★METHODS

KEY RESOURCES TABLE

REAGENT or RESOURCE	SOURCE	IDENTIFIER
Chemicals, Peptides, and Recombinant Proteins		
Polyethylenimine (PEI)	PolySciences	Cat#23966
Critical Commercial Assays		
Q5 Site-Directed Mutagenesis Kit	New England Biolabs	Cat#E0554S
Luciferase Assay Kit	Promega	Cat#1501
GenElute Plasmid Miniprep Kit	Sigma-Aldrich	PLN350
Deposited Data		
1610 full-length sequences	Dr. Andrew Rambaut	http://www.virological.org and https://github.com/ebov/space-time
Experimental Models: Cell Lines		
Bat kidney cells from Hypsignathus monstrosus	Kuhl et al., 2011	HypNi/1.1
Bat lung cells from Hypsignathus monstrosus	Kuhl et al., 2011	HypLu/45.1
Bat lung cells from Hippsideros abae	Kuhl et al., 2011	HipaLu/24.3
Bat kidney cells from Rousettus aegyptiacus	Kuhl et al., 2011	RoNi/7.1
Bat kidney cells from Epomops buettikoferi	Kuhl et al., 2011	EpoNi/22.1
Bat lung cells from Myotis daubentonii	Kuhl et al., 2011	MyDauLu/47.1
Human embryonic kidney cells	ECACC	HEK293T; RRID: CVCL_0063
Human bronchial epithelial cells	Reddel et al., 1989	BEAS-2B; RRID: CVCL_0168
Human lung alveolus cells	Smith, 1977	A549; RRID: CVCL_0023
Human hepatoma cell line	Nakabayashi et al., 1982	HuH7; RRID: CVCL_0336
Recombinant DNA		
GIN_1316_opt_pcDNA3.1(+): Codon optimized version of GenBank: AKG65286.1 in pCDNA3.1 plasmid vector	GenScript	GIN_1316_opt
pTG126 Luciferase encoding plasmid	François-Loïc Cosset	pTG126
phCMV-5349 MLV Gag/Pol-encoding plasmid	François-Loïc Cosset	phCMV-5349
Sequence-Based Reagents		
Primers for SDM, see Table S1	N/A	N/A
Software and Algorithms		
NEBaseChanger site directed mutagenesis software	New England Biolabs	http://nebasechanger.neb.com/
GTR+I+Γ model in PhyML	Guindon et al., 2010	N/A
PyMOL Molecular Graphics System, Version 1.8	Schrödinger	http://pymol.sourceforge.net; RRID: SCR_000305
PRISM	GraphPad Software	Version 6.05

CONTACT FOR REAGENT AND RESOURCE SHARING

Further information and requests for reagents may be directed to and fulfilled by the corresponding author Jonathan Ball (jonathan.ball@nottingham.ac.uk).

EXPERIMENTAL MODEL AND SUBJECT DETAILS

Cells

HEK293T, BEAS-2B, A549 and HuH7 cells were grown in Dulbecco's modified eagle medium (DMEM; Invitrogen), supplemented with 10% fetal bovine serum (Invitrogen), and 0.1mM nonessential amino acids (GIBCO) at 37°C and 5% CO_2. HypLu/45.1, HypNi/1.1, EpoNi/22.1, RoNi/7.1 cells were grown in DMEM with sodium pyruvate (Invitrogen), supplemented with 10% fetal bovine

serum (Invitrogen), and 0.1mM nonessential amino acids (GIBCO) at 37°C and 5% CO_2. Cell lines were tested to verify the absence of mycoplasma. No assays were performed to verify the identity of the cells in culture following receipt of the cells.

METHOD DETAILS

Phylogenetic analysis

Selectively advantageous mutations that spread through the viral population will fall on deeper branches on the phylogeny. Therefore, we determined whether amino acid changes that defined deep nodes (i.e., major clusters of lineages, particularly lineages A and B) on the EBOV Makona phylogeny resulted in more efficient human cell infection. Accordingly, a maximum likelihood phylogenetic tree was inferred using 1610 full-length sequences (sequence alignment of 18,996 nucleotides; dataset kindly provided by Dr. Andrew Rambaut, University of Edinburgh; available from Virological.org and https://github.com/ebov/space-time) representing EBOV Makona viruses sampled throughout the West African outbreak, utilizing the GTR+I+Γ model available in PhyML (Guindon et al., 2010) and NNI branch-swapping. Lineage-specific GP amino acid substitutions were mapped onto this phylogeny, and the robustness of individual nodes was provided by SH-like branch support values (Anisimova and Gascuel, 2006)

Construction of Ebola virus glycoprotein mutant panel

A codon-optimized version of *Zaire ebolavirus* GenBank: AKG65286.1, designated GIN_1316_opt, was commercially synthesized and cloned into pCDNA3.1(+) by GenScript. Oligonucleotides (see Key Resources Table and Table S1) were designed using NEBaseChanger (New England Biolabs) to introduce non-synonymous mutations into GIN_1316_opt by site directed mutagenesis (SDM) using the Q5 SDM kit (New England Biolabs). Mutant plasmid clones were prepared with a GenElute mini kit (Sigma-Aldrich), quantified by spectrophotometry (NanoDrop) and verified by Sanger sequencing (Source BioScience).

Transfection

Mutant plasmids were used to generate a panel of retroviral pseudoviruses (PVs). Transfections were performed as previously described (Mohan et al., 2015; Urbanowicz et al., 2016). Briefly, $1.2x10^6$ HEK293T cells were seeded overnight in a 10cm diameter Primaria coated dish (Corning) in 10mL of DMEM supplemented with non-essential amino acids and heat-inactivated FBS. Transfections were performed with 2 μg of phCMV MLV Gag/Pol, 2 μg of pTG126 Luciferase and 0.2 μg of EBOV GP, using 24 μL cationic polymer transfection reagent (Polyethylenimine), in the presence of Optimem (Invitrogen), and the media replaced with 10mL complete DMEM after 6 hr. Pseudovirus-containing supernatants were recovered after 72 hr, passed through a 0.45 μM filter and used either immediately or stored at 4°C for a maximum of one week. PVs were generated using a Murine Leukemia Virus (MLV) backbone rather than HIV backbone as our preliminary experiments indicated that the bat cells had an effective HIV cellular restriction factor (Besnier et al., 2003; Yap et al., 2014). This highlights the need to carefully consider the impact of cellular restriction when performing PV experiments in different cell lines.

Pseudovirus infection assays

Using the previously harvested PVs, 100 μL aliquots, in triplicate, were used to infect $1.5x10^4$ HuH7 cells or $2x10^4$ for all other cells (Key Resources Table) for 4 hr in a 96-well white plate (Corning). Following infection, 200 μL DMEM was added to the cells. Seventy-two hours following infection, media was discarded, cells lysed with 50 μL Cell Lysis Buffer (Promega) and luminescence assessed for each infection using a BMG Labtech FluoroStar Omega luminometer. PMT gain was set to 3600 and 50 μL of Promega luciferase substrate was injected immediately before a one second luminescence reading. Using this protocol negative control readings following addition of pseudoviruses bearing no glycoproteins routinely resulted in luminescence of between 0-100 Relative Light Units (RLU), dependent on the experiment. Each infection was performed in triplicate and the amount of infectivity for each mutant GP (measured in relative light units) was normalized to that observed for the initial EBOV Makona Kissidougou-C15 isolate sampled in March 2014. No normalization to MLV Gag p30 was undertaken as previous studies (Herrera et al., 2005) have highlighted that PV preparations contain a heterogeneous mix of core particles, GP-containing micro-vesicles and intact PV particles incorporating various molar ratios of GP, making standardization difficult. In contrast, we have used the same PV preparations to infect the various cells under study and have seen differences in infectivity in these different cells (bat versus human) using these same PV preps, meaning that the differences observed were a property of the cell line permissiveness rather than anything to do with the PV prep (i.e., the bat and human cells acts as reciprocal controls and increase in infectivity in one cell line and a concomitant decrease in the other is unlikely to arise because of PV heterogeneity). While we do not feel that these experiments are valuable in the comparative study that we performed, it is worth noting that the western blot analyses of PV particles in the accompanying manuscript (Diehl et al., 2016) shows no difference in expression levels for the various mutants analyzed.

Modeling

The structure illustrations were prepared using the PyMOL Molecular Graphics System, Version 1.8 Schrödinger, LLC (http://pymol.sourceforge.net).

QUANTIFICATION AND STATISTICAL ANALYSIS

Data are presented as mean ± SD unless otherwise indicated in figure legends. Experimental repeats are indicated in figures and figure legends. Data were analyzed using the repeated-measures one-way ANOVA with Dunnett's multiple comparison test unless otherwise indicated in figure legends. Correlations between infectivity observed in different cell lines were determined using Pearson correlation. Data analysis was not blinded. Differences in means were considered statistically significant at $p < 0.05$. Significance levels are: * $p < 0.05$; ** $p < 0.01$; *** $p < 0.001$; **** $p < 0.0001$; n.s., non-significant. Analyses were performed using the GraphPad PRISM 6.05 software.

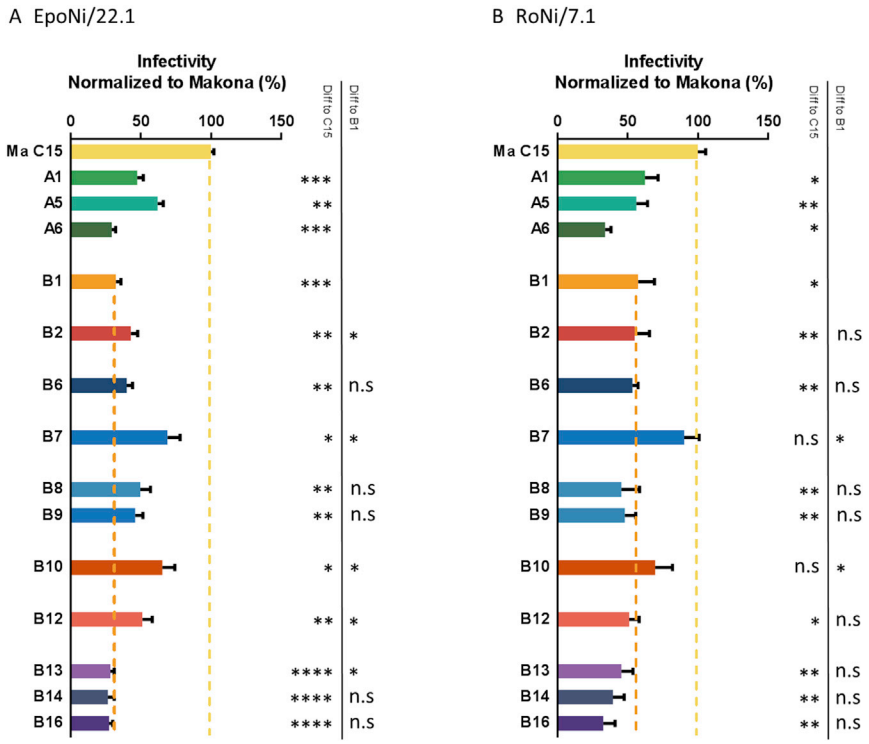

Figure S1. Infectivity of Pseudoviruses Supplemented with EBOV GP Mutants Observed in Kidney Cells from Two Different Fruit-Bat Species, Related to Figures 4 and S2

(A and B) Relative infectivity of each glycoprotein was expressed as a proportion (%) of that observed for the Kissidougou-C15 strain in *Epomops buettikoferi* kidney cells (EpoNi/22.1; A) and *Rousettus aegyptiacus* kidney cells (RoNi/7.1; B). Histogram bar colors correspond to the lineage color-coding shown in Figure 1. These data are the means ± 1 SD of three independent experiments, each performed in triplicate. Differences in the mean infectivity of each mutant compared to the Kissidougou-C15 EBOV strain and the lineage B viruses to the A82V mutant were assessed using repeated-measures one-way ANOVA with Dunnett's multiple comparison test and indicated in the table inset; * $p < 0.05$; ** $p < 0.01$; *** $p < 0.001$; n.s., not significant.

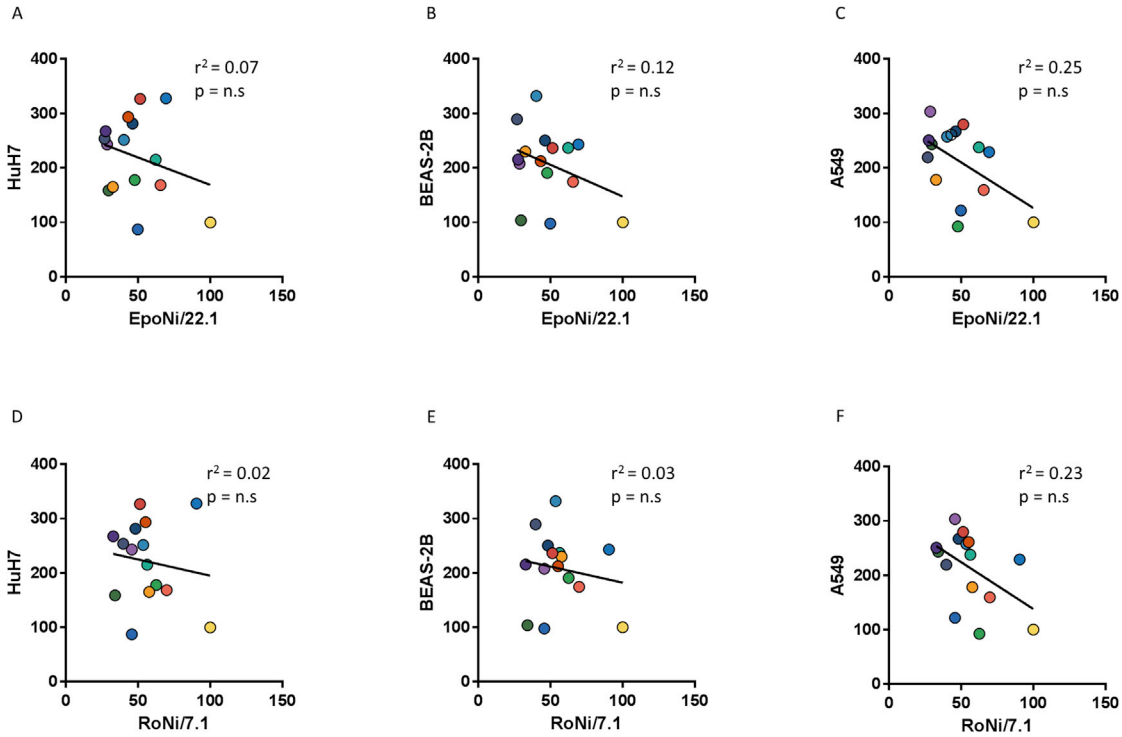

Figure S2. Negative Correlation of GP Mutant Infectivity in *Epomops Buettikoferi* Kidney, *Rousettus Aegyptiacus* Kidney, and Human Cells, Related to Figures 3 and S1

(A–F) Normalized infectivity data for each GP mutants were plotted for *Epomops buettikoferi* kidney cells (EpoNi/22.1) versus HuH7 (A), BEAS-2B (B), and A549 (C) and *Rousettus aegyptiacus* kidney cells (RoNi/7.1) versus HuH7 (D), BEAS-2B (E), and A549 (F). Infectivity data are the same as that shown in Figures 3 and S1. Correlations were determined using Pearson's correlation test.